Mineralogical Magazine, October 2015, Vol. 79(5), pp. 1123–1142

Fermiite, $Na_4(UO_2)(SO_4)_3{\cdot}3H_2O$ and oppenheimerite, $Na_2(UO_2)(SO_4)_2{\cdot}3H_2O$, two new uranyl sulfate minerals from the Blue Lizard mine, San Juan County, Utah, USA

Anthony R. Kampf[1,*], Jakub Plášil[2], Anatoly V. Kasatkin[3], Joe Marty[4] and Jiří Čejka[5]

[1] Mineral Sciences Department, Natural History Museum of Los Angeles County, 900 Exposition Boulevard, Los Angeles, CA 90007, USA
[2] Institute of Physics ASCR, v.v.i., Na Slovance 1999/2, 18221 Praha 8, Czech Republic
[3] Fersman Mineralogical Museum of Russian Academy of Sciences, Leninsky Prospekt 18-2, 119071 Moscow, Russia
[4] 5199 East Silver Oak Road, Salt Lake City, UT 84108, USA
[5] Department of Mineralogy and Petrology, National Museum, Cirkusová 1740, 193 00 Prague 9, Czech Republic

[*Received 4 January 2015; Accepted 27 January 2015; Associate Editor: S.J. Mills*]

ABSTRACT

The new minerals fermiite (IMA2014-068), $Na_4(UO_2)(SO_4)_3{\cdot}3H_2O$ and oppenheimerite (IMA2014-073), $Na_2(UO_2)(SO_4)_2{\cdot}3H_2O$, were found in the Blue Lizard mine, San Juan County, Utah, USA, where they occur together as secondary alteration phases in association with blödite, bluelizardite, chalcanthite, epsomite, gypsum, hexahydrite, kröhnkite, manganoblödite, sideronatrite, tamarugite and wetherillite.

Fermiite descriptive details: pale greenish-yellow prisms; transparent; vitreous lustre; bright greenish-white fluorescence; white streak; hardness (Mohs) 2½; brittle; conchoidal fracture; no cleavage; slightly deliquescent; easily soluble in RT H_2O; density$_{meas}$ = 3.23(2) g cm^{-3}; density$_{calc}$ = 3.313 g cm^{-3}. Optically, biaxial (+), $\alpha = 1.527(1)$, $\beta = 1.534(1)$, $\gamma = 1.567(1)$ (white light); $2V_{meas.} = 51(1)°$, $2V_{calc.} = 50°$; dispersion $r < v$, distinct. Pleochroism: X, Y = colourless, Z = pale greenish yellow; $X = Y < Z$. Energy dispersive spectroscopic (EDS) analyses yielded the empirical formula $Na_{3.88}(U_{1.05}O_2)(S_{0.99}O_4)_3(H_2O)_3$. Fermiite is orthorhombic, $Pmn2_1$, $a = 11.8407(12)$, $b = 7.8695(5)$, $c = 15.3255(19)$ Å, $V = 1428.0(2)$ Å^3 and $Z = 4$. The structure ($R_1 = 2.21\%$ for 1951 $I_o > 3\sigma I$) contains $[(UO_2)(SO_4)_3]$ chains that are linked by bonds involving five different Na–O polyhedra to form a framework. The mineral is named for Italian-American theoretical and experimental physicist Dr. Enrico Fermi (1901–1954).

Oppenheimerite descriptive details: pale greenish-yellow prisms; transparent; vitreous lustre; bright greenish-white fluorescence; white streak; hardness (Mohs) 2½; slightly sectile; three good cleavages, $\{1\bar{1}0\}$, $\{011\}$ and $\{101\}$; irregular fracture; slightly deliquescent; easily soluble in RT H_2O; density$_{calc}$ = 3.360 g cm^{-3}. Optically, biaxial (+), $\alpha = 1.537(1)$, $\beta = 1.555(1)$, $\gamma = 1.594(1)$ (white light); $2V_{meas.} = 72(2)°$, $2V_{calc.} = 70°$; dispersion is $r > v$, moderate, inclined; optical orientation: $X \approx \perp \{101\}$, $Z \approx [11\bar{1}]$; pleochroism: X very pale greenish yellow, Y pale greenish yellow, Z greenish yellow; $X < Y < Z$. EDS analyses yielded the empirical formula $Na_{1.94}(U_{0.97}O_2)(S_{1.02}O_4)_2(H_2O)_3$. Oppenheimerite is triclinic, $P\bar{1}$, $a = 7.9576(6)$, $b = 8.1952(6)$, $c = 9.8051(7)$ Å, $\alpha = 65.967(5)$, $\beta = 70.281(5)$, $\gamma = 84.516(6)°$, $V = 549.10(8)$ Å^3 and $Z = 2$. The structure ($R_1 = 3.07\%$ for 2337 $I_o > 3\sigma I$) contains $[(UO_2)(SO_4)_2(H_2O)]$ chains that are linked by bonds involving two different Na–O polyhedra to form a framework. The mineral is named for American theoretical physicist Dr. J. Robert Oppenheimer (1904–1967).

* E-mail: akampf@nhm.org
DOI: 10.1180/minmag.2015.079.5.8

Keywords: fermiite, oppenheimerite, new mineral, uranyl sulfate, crystal structure, Blue Lizard mine, Utah, USA.

Introduction

Assemblages of uranyl sulfate minerals are common in most uranium deposits, where they are formed by the weathering of primary uranium minerals, mainly uraninite, by acidic solutions derived from the decomposition of associated sulfides (Plášil, 2014). Over the last several years, we have been investigating a remarkable Na-rich uranyl sulfate assemblage in the inactive Blue Lizard uranium mine in southeast Utah. To date, our investigations have yielded six new uranyl sulfate minerals, belakovskiite (Kampf *et al*., 2014), bluelizardite (Plášil *et al.*, 2014), meisserite (Plášil *et al.*, 2013), plášilite (Kampf *et al*., 2015*a*), bobcookite (Kampf *et al*., 2015*b*) and wetherillite (Kampf *et al*., 2015*b*). The seventh and eighth new uranyl sulfates from this mine, fermiite and oppenheimerite, are described herein.

Fermiite (/′fer mi: ait/) is named in honour of Enrico Fermi (1901–1954). Dr Fermi, an Italian-American theoretical and experimental physicist, was best known for his work on the Manhattan Project during World War II, for which he led the team that in 1942 initiated the first artificial, self-sustaining nuclear chain reaction in an experimental reactor known as Chicago Pile-1, under the stands of Stagg Field at the University of Chicago. He is noted, as well, for his very significant contributions to the development of the quantum theory, nuclear and particle physics and statistical mechanics. Many scientific concepts, awards, institutions, etc. are named after Fermi, including the element fermium, the fermion (class of particles), the fermi (unit of measurement), the Enrico Fermi Award, the Enrico Fermi Institute, the Fermilab (Fermi National Accelerator Laboratory), the Fermi Gamma-ray Space Telescope and the Enrico Fermi Nuclear Generating Station.

Oppenheimerite (/′a:p ən hai mər ait/) is named in honour of J. Robert Oppenheimer (1904–1967). Dr Oppenheimer, an American theoretical physicist, was Professor of Physics concurrently at the University of California, Berkeley and the California Institute of Technology. He did important research in astrophysics, nuclear physics, spectroscopy and quantum field theory, but is best known for his work as scientific director of the Manhattan Project during World War II. After the war, he became an outspoken critic of the development of the hydrogen bomb.

The new minerals and their names were approved by the Commission on New Minerals, Nomenclature and Classification of the International Mineralogical Association (fermiite: IMA2014-068; oppenheimerite: IMA2014-073). The fermiite description is based on four cotype specimens. Three are deposited in the collections of the Natural History Museum of Los Angeles County, catalogue numbers 65546, 65547 and 65548, and one is housed in the collections of the Fersman Mineralogical Museum of the Russian Academy of Sciences, Moscow, Russia, catalogue number 94621. The description of oppenheimerite is also based on four cotype specimens. Three are deposited in the Natural History Museum of Los Angeles County, catalogue numbers 65549, 65550 and 65551, and one is housed in the collections of the Fersman Mineralogical Museum of the Russian Academy of Sciences, Moscow, Russia, catalogue number 94622.

Occurrence

Fermiite and oppenheimerite were found underground in the Blue Lizard mine, Red Canyon, White Canyon district, San Juan County, Utah, USA (37°33′26″N 110°17′44″W). The Blue Lizard mine is located ~72 km west of the town of Blanding, Utah, and ~22 km southeast of Good Hope Bay on Lake Powell. It is on the north side of Red Canyon and close to the Markey mine. Information on the history and geology of the deposit are provided by Kampf *et al*. (2015*b*) based largely on a report by Chenoweth (1993). Both fermiite and oppenheimerite have also been found at the nearby Green Lizard mine, also in Red Canyon, but the foregoing description is based only on material from the Blue Lizard mine, which is considered the type locality.

Fermiite and oppenheimerite are relatively rare minerals in the secondary uranyl sulfate mineral assemblage at the Blue Lizard mine. The two species occur together with other secondary minerals including blödite, bluelizardite (Plášil *et al.*, 2014), chalcanthite, epsomite, gypsum, hexahydrite, kröhnkite, manganoblödite (Kasatkin *et al*., 2013), sideronatrite, tamarugite and wetherillite (Kampf *et al*., 2015*b*). The bulk of the matrix is comprised of subhedral to euhedral, equant quartz crystals that are recrystallized counterparts of

FIG. 1. Fermiite crystals; field of view: 2 mm across.

the original grains of the sandstone. Other minerals remaining from the original sandstone include feldspar and rare almandine and zircon. Minerals related to the ore deposition include baryte, bornite, chalcopyrite, covellite, pyrite and uraninite. Other secondary minerals in the general assemblage include aluminocoquimbite, atacamite, belakovskiite (Kampf *et al*., 2014), blödite, bobcookite (Kampf *et al*., 2015*b*), brochantite, calcite, cobaltoblödite (Kasatkin *et al*., 2013), copiapite, coquimbite, cyanotrichite, d'ansite-(Mn), dickite, dietrichite, epsomite, ferrinatrite, gerhardtite, gordaite, halite, kieserite, kröhnkite, lishizhenite, meisserite (Plášil *et al*., 2013), metavoltine, natrozippeite, plášilite (Kampf *et al*., 2015*a*), pseudojohannite, rhomboclase, römerite, sideronatrite, tamarugite and other new minerals currently under investigation.

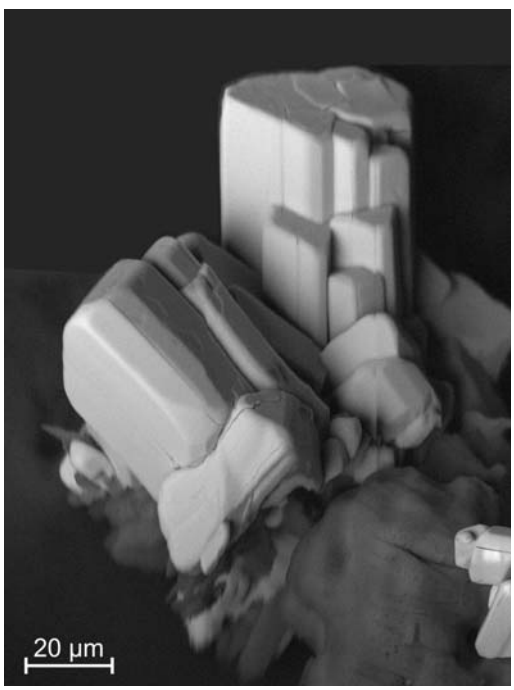

FIG. 2. Backscattered electron image of fermite crystals on hexahydrite.

Physical and optical properties

Fermiite

Fermiite commonly occurs in pale greenish-yellow prisms up to ~0.5 mm long, but is usually much smaller (Figs 1 to 3). Crystals occur as isolated individuals, subparallel intergrowths and irregular aggregates. Prisms are elongated on [010] and exhibit the forms {010}, {001}, {00$\bar{1}$}, {110}, {011}, {0$\bar{1}\bar{1}$}, {101} and {$\bar{1}$0$\bar{1}$}. Penetration twinning by 180° rotation on [010] was observed.

Crystals are transparent with a vitreous lustre. The mineral has white streak. The mineral fluoresces bright greenish white under both longwave and shortwave UV. The Mohs hardness is ~2½. Crystals are brittle with no cleavage and conchoidal fracture. The mineral is slightly deliquescent and is easily soluble in room temperature H_2O. The density measured by floatation in a mixture of methylene iodide and acetone is 3.23(2) g cm^{-3}. The calculated densities are 3.313 g cm^{-3} based on the empirical formula and 3.275 g cm^{-3} based on the ideal formula.

Optically, fermiite is biaxial (+), with α = 1.527(1), β = 1.534(1), γ = 1.567(1) (measured in white light). The 2V measured directly on a spindle

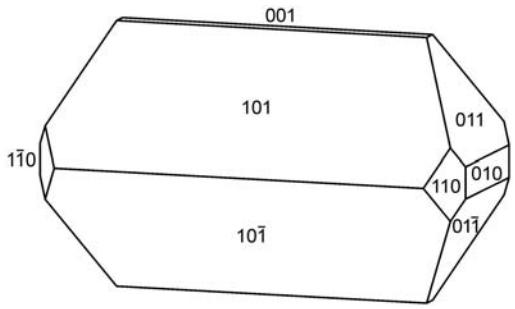

FIG. 3. Crystal drawing of fermiite; clinographic projection in standard orientation.

FIG. 4. Oppenheimerite with hexahydrite (white) on blödite; field of view 5 mm across.

stage is 51(1)°; the calculated 2V is 50°. Dispersion is $r < v$, distinct. Pleochroism is X, Y = colourless, Z = pale greenish yellow; $X = Y < Z$. The optical orientation is $X = b$, $Y = c$, $Z = a$.

Oppenheimerite

Oppenheimerite commonly occurs as pale greenish-yellow prisms in subparallel intergrowths up to several mm across with surfaces consisting of numerous small stepped faces (Figs 4 to 6). Prisms are elongated on $[11\bar{1}]$ and exhibit the forms {100}, {010}, {001}, {101}, {011}, {110} and $\{10\bar{1}\}$. No twinning was observed.

Crystals are transparent with a vitreous lustre. The mineral has a white streak. The mineral fluoresces bright greenish white under both long-wave and shortwave UV. The Mohs hardness is ~2½. Crystals are slightly sectile with three good cleavages: $\{1\bar{1}0\}$, {001} and {101}. The fracture is irregular. The mineral is easily soluble in room temperature H_2O. Crystals sink in pure methylene iodide (density = 3.325 g cm^{-3}). Because crystals are soluble in Clerici solution, it was not possible to measure the density of oppenheimerite. The calculated densities are 3.360 g cm^{-3} based on the empirical formula and 3.400 g cm^{-3} based on the ideal formula.

Optically, oppenheimerite is biaxial (+), with α = 1.537(1), β = 1.555(1), γ = 1.594(1) (measured in white light). The 2V measured directly on a spindle stage is 72(2)°; the calculated 2V is 70°. Dispersion is $r > v$, moderate, inclined. Pleochroism is X very pale greenish yellow, Y pale greenish yellow, Z greenish yellow; $X < Y < Z$. The optical orientation is $X \approx \perp$ {101}, $Z \approx [11\bar{1}]$.

Raman spectroscopy

The Raman spectra of fermiite and oppenheimerite were recorded on a Thermo-Scientific DXR Raman

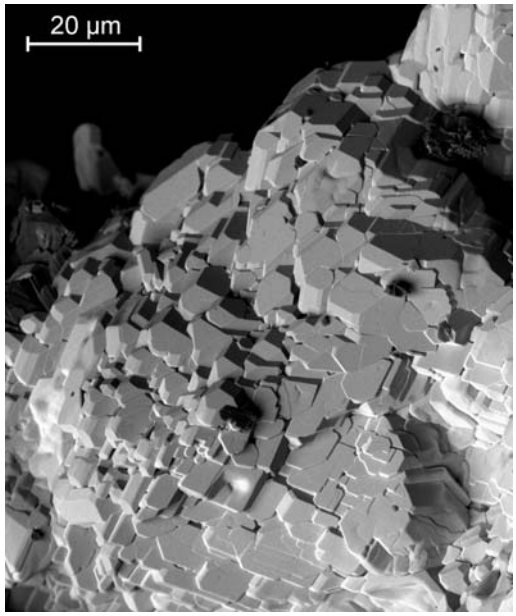

FIG. 5. Backscattered electron image of a subparallel intergrowth of oppenheimerite crystals.

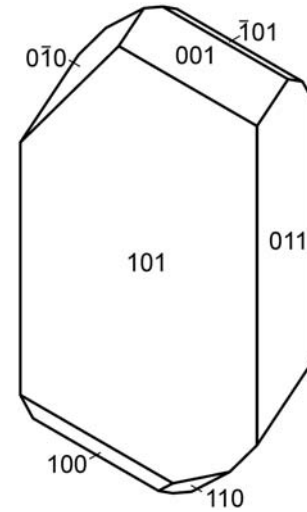

FIG. 6. Crystal drawing of oppenheimerite; clinographic projection in nonstandard orientation, $[11\bar{1}]$ vertical.

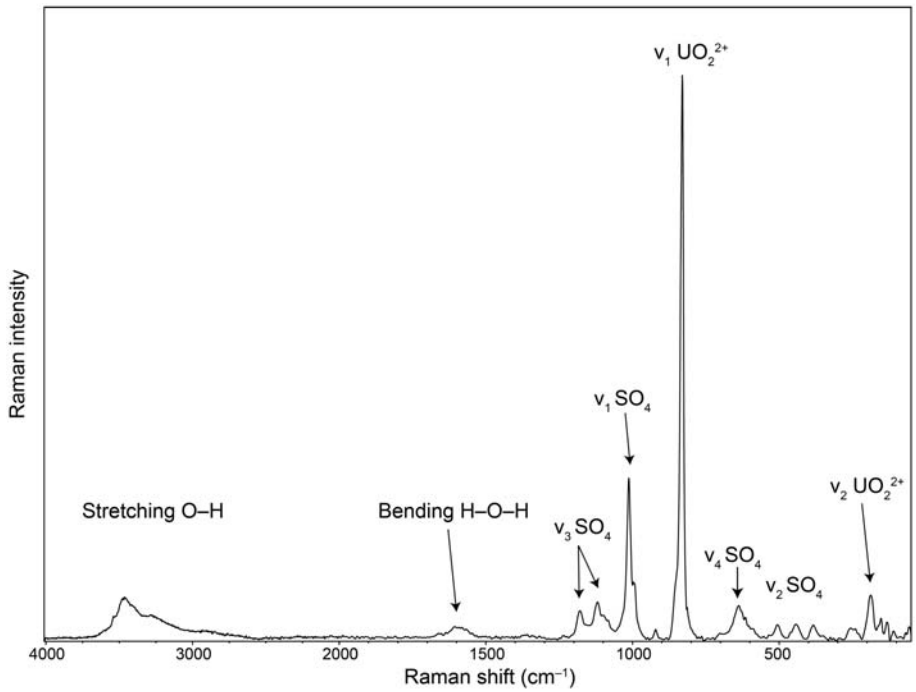

FIG. 7. The Raman spectrum of fermiite measured with a 532 nm laser.

microscope interfaced to an Olympus microscope (50× objective). The spectrometer was calibrated by a software-controlled calibration procedure (within Omnic 8 software) using multiple neon emission lines (wavelength calibration), multiple polystyrene Raman bands (laser frequency calibration) and standardized white light sources (intensity calibration). Spectral manipulation such as background correction and band-component analysis was undertaken with Omnic 8 software.

Fermiite

The Raman spectrum of fermiite is shown in Fig. 7. Bands at 3540, 3465 and 3285 cm^{-1} were assigned to ν(OH) stretching vibrations of structurally inequivalent H_2O. Inferred O–H···O hydrogen bond lengths lie approximately in the range 2.75–2.98 Å (Libowitzky, 1999). A weak, broad band with a maximum at 1606 cm^{-1} is connected with $\nu_2(\delta)$ bending vibrations of H_2O. Weak bands with shoulders at 1228, 1180, 1120, 1104 and 1080 cm^{-1} are attributed to triply degenerate $\nu_3(SO_4)^{2-}$ antisymmetric stretching and those at 1013 and 996 cm^{-1} to $\nu_1(SO_4)^{2-}$ symmetric stretching vibrations.

A weak band at 922 cm^{-1} is attributed to $\nu_3(UO_2)^{2+}$ antisymmetric stretching. A very strong band at 830 cm^{-1} is assigned to the $\nu_1(UO_2)^{2+}$ symmetric stretching. Two shoulders at 860 and 813 cm^{-1} might be related to the libration modes of water molecules or to $\nu_1(UO_2)^{2+}$ symmetric stretching vibration. While the observed wavenumber of 830 cm^{-1} is a reasonable value for the $\nu_1(UO_2)^{2+}$ symmetric stretching vibration, as observed recently in the case of the minerals bobcookite and wetherillite (Kampf *et al.*, 2015*b*), the other two numbers, 860 and 813 cm^{-1}, are slightly larger and smaller than one might expect. However, in the crystal structure of fermiite, there are two symmetrically independent U atoms, which can produce splitting of the stretching modes. U–O bond lengths, inferred from observed wavenumbers of the ν_3 and $\nu_1(UO_2)^{2+}$ vibrations are (Å/cm^{-1}) 1.77/921 and 1.78/830 and probably also 1.75/860 and 1.79/813, if the two shoulders are taken into account (Bartlett and Cooney, 1989). However, two shoulders at 860 and 813 cm^{-1} together with a very weak band at 701 cm^{-1} may be assigned to libration modes of water molecules.

Weak bands at 638, 616 and 583 cm^{-1} are attributed to triply degenerate $\nu_4(\delta)(SO_4)^{2-}$ bending and those at

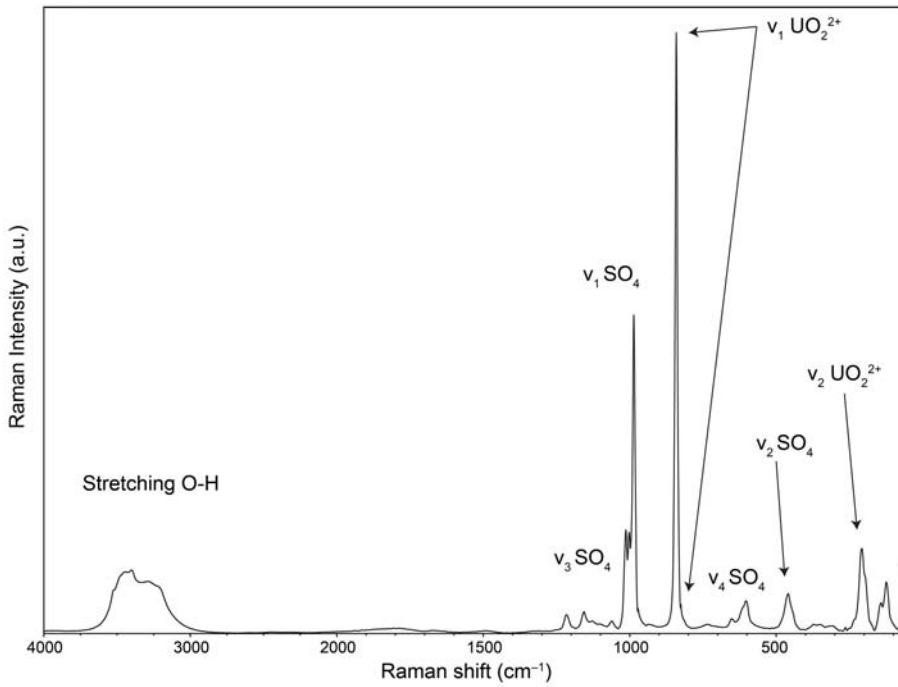

FIG. 8. The Raman spectrum of oppenheimerite measured with a 532 nm laser.

506, 443 and 384 cm^{-1} to doubly degenerate $\nu_2(\delta)(SO_4)^{2-}$ bending. The band at 384 cm^{-1} may be connected with $\nu(U–O_{equatorial})$ stretching vibrations or with Na–O stretching vibrations, similar to the assignments for K–O and Na–O stretches observed for U^{6+} compounds (e.g. Volkovich *et al*., 1998; Plášil *et al*., 2010; Kampf *et al*., 2015). Bands at 239 and 256 cm^{-1} are attributed to doubly degenerate $\nu_2(\delta)(UO_2)^{2+}$ vibrations. Remaining bands (188, 163, 153, 132, 110 and 55 cm^{-1}) may be assigned to lattice vibrations.

Oppenheimerite

The Raman spectrum of oppenheimerite is shown in Fig. 8. Raman bands at 3526, 3400 and 3218 cm^{-1} are assigned to the ν(O–H) stretching vibrations of structurally non-equivalent H_2O molecules. Inferred O–H···O hydrogen bond–lengths (Libowitzky, 1999) lie approximately within the range 2.70–2.95 Å. A couple of broad peaks at ~1700 cm^{-1} are artifacts; however, the $\nu_2(\delta)$ bending vibration of H_2O, with a low Raman intensity, should occur at ~1600 cm^{-1}. Weak bands with shoulders at 1215, 1156 and 1060 cm^{-1} are connected to the triply degenerate $\nu_3(SO_4)^{2-}$ antisymmetric stretching vibrations and those at 1013, 1002, 986 and 970 cm^{-1} are connected with the $\nu_1(SO_4)^{2-}$ symmetric stretching vibrations. No band assignable to the antisymmetric stretching vibration of $(UO_2)^{2+}$ was observed. A very strong band at 841 cm^{-1} with a shoulder at 825 cm^{-1} was assigned to the $\nu_1(UO_2)^{2+}$ symmetric stretching vibration. Approximate U–O bond lengths, inferred from these wavenumbers of the $\nu_1(UO_2)^{2+}$ vibrations, are (Å/cm^{-1}) 1.770/841 and 1.786/825 (Bartlett and Cooney, 1989). These values are in agreement with the U–O uranyl bond lengths obtained from the X-ray data, 1.765(4) and 1.774(4) Å. Weak bands at 651 and 603 cm^{-1} were assigned to the triply degenerate $\nu_4(\delta)(SO_4)^{2-}$ bending vibration and the band at 459 and a shoulder at 378 cm^{-1} were assigned to the doubly degenerate $\nu_2(\delta)(SO_4)^{2-}$ bending vibration. The shoulder at 378 cm^{-1}, together with that at 345 cm^{-1}, may be attributed to $\nu(U–O_{equatorial})$ stretching vibrations or to Na–O stretching vibrations similar to the assignments for K–O and Na–O stretches observed for U^{6+} compounds (e.g. Volkovich *et al*., 1998; Plášil *et al*., 2010; Kampf

TABLE 1. Chemical analyses for fermiite and oppenheimerite.

Constituent	wt.%	Range	S.D.	Probe standard
Fermiite				
Na_2O	17.10	15.65–18.05	0.87	Chkalovite
UO_3	42.77	40.88–45.35	1.69	syn. UO_2
SO_3	33.85	32.64–35.49	1.00	syn. ZnS
H_2O*	7.70			
Total	101.42			
Oppenheimerite				
Na_2O	10.94	9.12–11.92	0.98	Chkalovite
UO_3	50.77	48.74–54.52	2.03	syn. UO_2
SO_3	29.75	27.88–31.54	1.19	syn. ZnS
$H_2O^{\S}$	9.85			
Total	101.31			

S.D. – standard deviation; syn. – synthetic.
* Calculated by stoichiometry on the basis of 17 O a.p.f.u.
§ Calculated by stoichiometry on the basis of 13 O a.p.f.u.

et al., 2015). The band at 207 cm^{-1} was assigned to the doubly degenerate $\nu_2(\delta)(UO_2)^{2+}$ vibration. Remaining bands (188, 163, 153, 132, 110 and 55 cm^{-1}) may be assigned to lattice modes.

Composition

The chemical compositions of fermiite and oppenheimerite were determined using a CamScan4D scanning electron microscope (SEM) equipped with an Oxford Link ISIS energy-dispersive X-ray spectrometer. An operating voltage of 20 kV was used with a beam current of 1 nA and a 1 μm beam diameter. The EDS mode on the SEM was chosen for the analyses instead of the wavelength dispersive spectroscopy (WDS) mode on the electron microprobe because of the instability of the phases under the electron beam caused by the high contents of both Na and H_2O. Attempts to use the WDS mode were unsuccessful because of significant decomposition of the minerals after several seconds under the electron beam. The H_2O contents were not determined directly because of the scarcity of pure material. Instead, the H_2O contents were calculated by stoichiometry on the basis of the crystal structure determinations. No other elements with atomic numbers >8 were observed. Analytical data are given in Table 1.

The empirical formula of fermiite, calculated as the mean of six representative spot analyses, is $Na_{3.88}U_{1.05}S_{2.97}O_{17.00}H_{6.00}$, or $Na_{3.88}(U_{1.05}O_2)(S_{0.99}O_4)_3(H_2O)_3$. (based on 17 O atoms per formula unit (a.p.f.u.)). The simplified formula is $Na_4(UO_2)(SO_4)_3(H_2O)_3$ which requires Na_2O 17.60, UO_3 40.62, SO_3 34.11 and H_2O 7.67, total 100.00 wt.%.

The empirical formula of oppenheimerite, calculated as the mean of 12 representative spot analyses, is $Na_{1.94}U_{0.97}S_{2.04}O_{13.00}H_{6.00}$, or $Na_{1.94}(U_{0.97}O_2)(S_{1.02}O_4)_2(H_2O)_3$.(based on 13 O a.p.f.u.). The simplified formula is $Na_2(UO_2)(SO_4)_2(H_2O)_3$ which requires Na_2O 11.03, UO_3 50.80, SO_3 28.55 and H_2O 9.62, total 100.00 wt.%.

The Gladstone-Dale compatibility index $1 - (K_P/K_C)$ for the empirical formulas of fermiite and oppenheimerite are 0.008 and –0.015, respectively, in both cases in the range of superior compatibility (Mandarino, 2007). As noted by Kampf *et al*. (2015*a*), Gladstone-Dale calculations for uranyl sulfates should utilize $k(UO_3) = 0.118$, as provided by Mandarino (1976).

X-ray crystallography and structure refinement

Powder X-ray studies were carried out using a Rigaku R-Axis Rapid II curved imaging plate microdiffractometer, with monochromatized Mo*K*α radiation (λ = 0.71075 Å). A Gandolfi-like motion on the φ and ω axes was used to randomize the sample and the *d* spacings and intensities observed were derived by profile fitting using *JADE 2010* software (Materials Data, Inc.). The powder data presented in Table 2 show good agreement with the patterns calculated from the structure

TABLE 2. Powder X-ray data for fermiite and oppenheimerite.

Fermiite I_{obs}	d_{obs}	d_{calc}	I_{calc}	*hkl*
33	9.42	9.3699	33	1 0 1
		7.8695	3	0 1 0
43	7.71	7.6627	44	0 0 2
100	7.01	7.0005	100	0 1 1
49	6.00	6.0261	24	1 1 1
		5.9204	23	2 0 0
13	5.50	5.4900	13	0 1 2
2	5.04	4.9807	2	1 1 2
42	4.70	4.6906	17	1 0 3
		4.6849	25	2 0 2
13	4.53	4.5205	13	2 1 1
17	4.30	4.2848	15	0 1 3
13	4.018	4.0291	9	1 1 3
15	3.910	3.9348	13	0 2 0
		3.8222	6	3 0 1
		3.8111	5	0 2 1
17	3.759	3.7340	11	1 2 0
		3.6279	3	1 2 1
85	3.476	3.5003	10	0 2 2
		3.4711	51	2 1 3
		3.4448	5	0 1 4
		3.4381	17	3 1 1
55	3.336	3.3567	24	1 2 2
		3.3077	27	1 1 4
22	3.243	3.2770	11	2 2 0
		3.2166	8	2 0 4
		3.2047	11	3 1 2
57	3.131	3.1233	31	3 0 3
		3.1173	21	0 2 3
32	2.987	3.0145	11	1 2 3
		2.9775	4	2 1 4
		2.9673	6	1 0 5
		2.9602	16	4 0 0
46	2.762	2.7866	15	3 2 0
		2.7613	13	4 0 2
		2.7416	6	3 2 1
		2.7264	14	4 1 1

I_{obs}	d_{obs}	d_{calc}	I_{calc}	*hkl*
10	2.301	2.3138	3	3 1 5
		2.2895	10	1 3 3
18	2.256	2.2603	2	4 2 2
		2.2536	5	3 2 4
		2.2476	2	2 1 6
		2.2433	4	5 1 1
		2.2385	7	2 2 5
31	2.164	2.1645	10	0 3 4
		2.1628	9	3 3 1
		2.1529	6	1 0 7
		2.1485	4	5 0 3
		2.1465	2	4 2 3
16	2.068	2.0727	2	5 1 3
		2.0689	7	3 1 6
		2.0619	7	3 2 5
12	2.023	2.0329	7	2 3 4
		2.0290	3	5 2 0
		2.0087	5	3 3 3
30	1.9659	1.9869	2	2 1 7
		1.9735	8	6 0 0
		1.9614	11	5 2 2
		1.9515	6	5 1 4
		1.9408	6	1 4 0
21	1.9184	1.9145	4	3 0 7
		1.9131	6	0 2 7
		1.9111	2	6 0 2
		1.9018	2	4 3 2
27	1.8849	1.8994	4	6 1 1
		1.8887	7	1 2 7
		1.8857	2	5 2 3
		1.8814	2	1 4 2
		1.8740	6	5 0 5
		1.8727	7	4 2 5
12	1.8311	1.8388	2	1 1 8
		1.8359	2	0 4 3
		1.8300	3	0 3 6
		1.8205	6	2 2 7

I_{obs}	d_{obs}	d_{calc}	I_{calc}	*hkl*
11	1.6614	1.6674	3	6 2 3
		1.6621	3	5 3 3
		1.6557	3	0 4 5
14	1.6098	1.6442	2	7 1 1
		1.6165	3	7 1 2
		1.6076	3	5 0 7
		1.6068	2	4 2 7
		1.6058	2	7 0 3
		1.6022	4	2 1 9
		1.5945	4	2 4 5
16	1.5613	1.5657	3	0 5 1
		1.5635	2	3 0 9
		1.5602	3	4 4 3
		1.5566	4	4 3 6
14	1.5267	1.5289	3	6 2 5
		1.5248	2	5 3 5
		1.5230	3	7 2 2
		1.5184	2	7 1 4
		1.5136	3	2 5 1
		1.5110	2	2 2 9
15	1.4933	1.4968	4	2 3 8
		1.4921	2	1 5 3
		1.4882	2	5 2 7
		1.4867	3	7 2 3
		1.4836	2	2 0 10
16	1.4562	1.4634	3	5 1 8
		1.4583	3	6 3 4
		1.4553	2	3 5 1
		1.4530	3	3 2 9
		1.4481	2	8 1 1
		1.4450	3	4 4 5
15	1.4207	1.4360	3	3 5 2
		1.4206	7	2 4 7
		1.4178	3	1 2 10
		1.4155	3	7 3 1
		1.4075	2	5 4 4
		1.4057	2	3 1 10

20	2.610	2.6741	4	1 2 4
		2.6188	8	3 2 2
		2.5953	9	3 1 4
8	2.519	2.5724	5	2 1 5
		2.5260	6	1 3 1
		2.4903	3	2 2 4
21	2.444	2.4818	2	0 3 2
		2.4463	11	3 2 3
		2.4355	2	4 1 3
15	2.381	2.4180	9	0 2 5
		2.3799	10	1 1 6
		2.3691	2	1 2 5
		2.3655	5	4 2 0
6	1.7964	1.7931	6	5 2 4
		1.7756	2	2 1 8
26	1.7541	1.7608	4	3 4 0
		1.7536	4	2 4 3
		1.7484	9	2 3 6
		1.7472	3	4 3 4
		1.7463	4	5 3 1
19	1.7186	1.7313	3	1 4 4
		1.7191	3	6 2 2
		1.7160	10	3 4 2
17	1.6942	1.7045	2	1 2 8
		1.6958	11	5 1 6
		1.6855	3	1 0 9
		1.6835	3	3 1 8
11	1.3916	1.3990	3	8 1 3
		1.3882	3	2 2 10
		1.3840	2	4 5 1
		1.3825	2	5 0 9
13	1.3706	1.3736	2	6 2 7
		1.3711	2	4 3 8
		1.3659	2	3 5 4
7	1.3445	1.3569	2	5 4 5
		1.3429	2	3 2 10
		1.3419	3	6 3 6
		1.3365	2	2 1 11

Oppenheimerite

I_{obs}	d_{obs}	d_{calc}	I_{calc}	*hkl*
5	8.49	8.4587	5	0 0 1
31	7.29	7.4759	18	0 1 0
		7.2148	47	0 1 1
73	6.85	6.8257	100	1 0 1
11	5.92	5.9298	14	1 1 1
47	5.39	5.4220	92	$\bar{1}$ 1 0
26	5.14	5.1643	25	1 1 0
27	4.817	4.8671	27	$\bar{1}$ 0 1
		4.7390	16	0 $\bar{1}$ 1
		4.6773	9	$\bar{1}$ 1 1
16	4.567	4.5416	18	0 1 2
21	2.554	2.5842	6	1 3 1
		2.5821	5	2 2 0
		2.5569	12	$\bar{1}$ 1 3
		2.5433	3	2 $\bar{2}$ 1
		2.5161	12	$\bar{2}$ 1 2
9	2.470	2.4996	6	$\bar{1}$ 3 1
		2.4920	4	0 3 0
		2.4629	4	1 3 3
		2.4476	3	$\bar{1}$ 2 3
		2.4326	5	1 1 4
		2.4012	3	$\bar{3}$ 1 0
12	1.9142	1.9228	3	4 1 1
		1.9183	3	1 1 5
		1.9063	4	2 1 5
		1.8996	4	2 $\bar{1}$ 4
		1.8935	5	$\bar{3}$ 0 2
16	1.8719	1.8798	6	$\bar{1}$ 0 4
		1.8742	6	3 3 4
		1.8705	3	4 0 0
		1.8669	7	$\bar{1}$ 3 4
		1.8588	6	$\bar{3}$ 2 2
		1.8501	5	0 $\bar{1}$ 4

(continued)

TABLE 2 (*contd.*)

7	4.352	4.3430	24	1 0 2
29	4.253	4.2293	21	0 0 2
22	4.065	4.0746	39	0 2 1
		3.7477	4	1 2 1
43	3.700	3.7410	22	2 0 0
		3.6912	20	2 1 1
		3.6636	5	$\bar{1}\,\bar{1}$ 1
21	3.593	3.6074	11	0 2 2
		3.5935	20	1 2 2
		3.4940	12	2 1 2
19	3.420	3.4109	34	$\bar{1}$ 2 0
100	3.257	3.3014	27	2 $\bar{1}$ 1
		3.2806	23	1 2 0
		3.2585	18	1 1 3
		3.2527	46	$\bar{1}$ 0 2
		3.1764	9	0 $\bar{1}$ 2
8	3.086	3.0689	11	$\bar{2}$ 0 1
		3.0034	3	0 $\bar{2}$ 1
		2.9930	7	1 2 3
24	2.973	2.9884	4	$\bar{1}$ 2 2
		2.9811	13	1 0 3
		2.9649	6	2 2 2
26	2.904	2.9124	23	2 2 1
9	2.844	2.8699	19	0 2 3
		2.8196	9	0 0 3
		2.7110	3	$\bar{2}$ 2 0
33	2.669	2.6961	13	2 2 3
		2.6777	8	$\bar{1}\,\bar{1}$ 2
		2.6706	8	$\bar{2}$ $\bar{1}$ 1
		2.6632	4	0 3 2
		2.6483	8	$\bar{1}$ $\bar{2}$ 1
		2.6387	6	3 0 1
		2.3989	3	1 2 4
		2.3920	3	$\bar{1}$ 0 3
28	2.346	2.3681	7	3 1 3
		2.3480	10	2 3 2
		2.3388	3	2 1 4
		2.3320	8	3 1 0
		2.3199	8	3 2 2
		2.3102	4	2 $\bar{1}$ 3
15	2.281	2.2981	4	2 2 4
		2.2888	3	0 1 4
		2.2798	6	3 $\bar{1}$ 2
		2.2752	3	3 0 3
		2.2708	4	0 2 4
		2.2362	3	1 0 4
		2.2300	6	2 $\bar{2}$ 2
		2.2039	3	$\bar{3}$ 1 1
11	2.151	2.1668	4	0 $\bar{3}$ 1
		2.1599	8	1 3 4
		2.1554	4	1 $\bar{3}$ 1
		2.1539	3	$\bar{2}$ $\bar{1}$ 2
6	2.115	2.1222	17	$\bar{2}$ 3 0
		2.0849	3	3 $\bar{2}$ 1
		2.0744	5	$\bar{1}\,\bar{1}$ 3
20	2.0291	2.0385	10	3 2 4
		2.0373	3	0 4 2
		2.0289	7	2 3 0
		2.0265	3	$\bar{2}$ 3 2
		2.0203	3	1 4 2
		2.0060	3	$\bar{1}$ 1 4
		2.0007	4	$\bar{1}$ 2 4
16	1.9653	1.9847	3	1 4 3
		1.9766	3	3 3 3
		1.9743	3	1 $\bar{2}$ 3
		1.9678	3	4 1 2
		1.9631	3	$\bar{2}$ 0 3
		1.9616	3	3 0 4
		1.9467	10	1 2 5
13	1.8320	1.8375	3	$\bar{2}$ 3 3
		1.8357	5	-4 1 0
		1.8344	3	$\bar{1}$ 4 0
		1.8318	5	$\bar{2}\,\bar{2}$ 2
		1.8191	4	$\bar{1}$ 4 3
		1.8137	3	0 1 5
22	1.7817	1.7968	7	2 4 4
		1.7869	8	$\bar{3}$ $\bar{2}$ 1
		1.7839	3	2 4 1
8	1.7349	1.7488	3	3 $\bar{3}$ 1
		1.7463	3	$\bar{2}$ 4 1
		1.7401	4	3 $\bar{2}$ 3
		1.7252	4	4 $\bar{1}$ 3
		1.7233	4	$\bar{1}$ $\bar{3}$ 2
9	1.7018	1.7118	6	4 $\bar{2}$ 1
		1.6943	4	$\bar{3}$ 3 2
		1.6917	3	0 0 5
		1.6792	3	$\bar{3}$ 1 3
		1.6659	3	3 4 2
8	1.6334	1.6559	5	4 3 2
		1.6360	3	-4 2 1
		1.6292	3	2 2 6
		1.6263	3	$\bar{2}$ 0 4
		1.6248	3	-4 $\bar{1}$ 1
		1.6170	3	1 5 2
		1.5914	3	1 $\bar{1}$ 5
9	1.5727	1.5851	3	0 5 1
		1.5755	3	1 5 4
		1.5645	6	3 4 5
9	1.5319	1.5379	3	0 2 6
		1.5318	6	$\bar{3}$ 4 0
		1.5241	3	3 $\bar{1}$ 5

For fermiite only calculated lines with $I > 1$ are shown; for oppenheimerite only calculated lines with $I > 2$ are shown.

TABLE 3. Data collection and structure refinement details for fermiite and oppenheimerite.

	Fermiite	Oppenheimerite
Diffractometer	Oxford Diffraction Gemini with Atlas detector	Rigaku R-Axis Rapid II
X-ray radiation/power	MoK_α (λ = 0.71075 Å)	MoK_α (λ = 0.71075 Å)
X-ray power	50 kV, 30 mA	50 kV, 40 mA
Temperature	293(2) K	298(2) K
Structural formula	$Na_4(H_2O)_3[(UO_2)(SO_4)_3]$	$Na_2(H_2O)_2[(UO_2)(SO_4)_2(H_2O)]$
Space group	$Pmn2_1$	$P\bar{1}$
Unit-cell dimensions	a = 11.8407(12) Å	a = 7.9576(6) Å
	b = 7.8695(5) Å	b = 8.1952(6) Å
	c = 15.3255(19) Å	c = 9.8051(7) Å
		α = 65.967(5)°
		β = 70.281(5)°
		γ = 84.516(6)°
V	1428.0(2) Å^3	549.10(8) Å^3
Z	4	2
Density (for above formula)	3.247 g cm^{-3}	3.400 g cm^{-3}
Absorption coefficient	12.02 mm^{-1}	15.31 mm^{-1}
F(000)	1280	500
Crystal size (μm)	54 × 52 × 17	150 × 80 × 55
θ range (°)	2.91 to 27.86	3.44 to 27.48
Index ranges	$0 \leq h \leq 14$	$-10 \leq h \leq 10$
	$0 \leq k \leq 10$	$-10 \leq k \leq 10$
	$-16 \leq l \leq 19$	$-12 \leq l \leq 12$
Reflections collected/unique	8131/2359; R_{int} = 0.043	10,297/2491; R_{int} = 0.056
Reflections with $I_o > 3\sigma I$	1951	2337
Completeness to θ_{max}	85%	99%
Refinement method	Full-matrix least-squares on F^2	Full-matrix least-squares on F^2
Parameters refined	251	163
Goof	1.03	1.31
Final R indices [$F_o > 4\sigma(F)$]	R_1 = 0.0221, wR_2 = 0.0408	R_1 = 0.0307, wR_2 = 0.0762
R indices (all data)	R_1 = 0.0321, wR_2 = 0.0447	R_1 = 0.0320, wR_2 = 0.0772
Absolute structure parameter	0.148(11)	
Weighting scheme, weights	σ, $w = 1/(\sigma^2(I) + 0.0004I^2$	σ, $w = 1/(\sigma^2(I) + 0.0004I^2$
Largest diff. peak/hole	+1.09/–0.86 e A^{-3}	+2.05/–1.35 e A^{-3}

determinations. Unit-cell parameters refined from the powder data using *JADE 2010* with whole pattern fitting are for fermiite: a = 11.8867(6), b = 7.8783(4), c = 15.3856(9) Å and V = 1440.8(1) Å^3; and for oppenheimerite: a = 7.962(2), b = 8.178(2), c = 9.796(2) Å, α = 66.116(9), β = 70.342(8), γ = 84.510(6)° and V = 548.6(2) Å^3.

The single-crystal structure data for fermiite were collected on an Oxford Diffraction Gemini single-crystal diffractometer with an Atlas CCD detector using monochromatized Mo$K\alpha$ radiation and were processed using the Agilent Technologies *CrysAlis* software package. The Gaussian correction for absorption was applied using the routine in *Jana2006* software (Petříček *et al.*, 2014) taking into account the crystal shape, refined utilizing the *X-SHAPE* software (Stoe & Cie GmbH). The fermiite structure was solved by the charge-flipping algorithm (Palatinus, 2013) implemented in the *Superflip* program (Palatinus and Chapuis, 2007). The somewhat smaller cell parameters for fermiite obtained in the single-crystal study (Table 3) as compared to those from the powder data (above) is attributed to different instrumentation. The fermiite single-crystal cell obtained on the Rigaku R-Axis Rapid II diffractometer was almost identical to that from the powder study on the same instrument.

The data for oppenheimerite were collected on a Rigaku R-Axis Rapid II curved imaging plate microdiffractometer, also using monochromatized Mo$K\alpha$ radiation. The oppenheimerite data were processed using the Rigaku *CrystalClear* software package and an empirical (multi-scan) correction was applied using the *ABSCOR* program (Higashi,

TABLE 4. Atom coordinates and displacement parameters (Å^2) for fermiite and oppenheimerite.

Fermiite	x/a	y/b	z/c	U_{eq}	U^{11}	U^{22}	U^{33}	U^{23}	U^{13}	U^{12}
U1	0.5	0.17284(7)	0.35598(2)	0.0104(2)	0.0099(5)	0.0101(3)	0.0113(4)	0	0	–0.0013(3)
U2	0	0.32352(7)	0.43882(2)	0.0094(2)	0.0073(5)	0.0098(3)	0.0112(4)	0	0	0.0006(3)
S1	0	0.2514(5)	–0.2447(3)	0.0120(13)	0.017(3)	0.0096(19)	0.0094(19)	0	0	–0.0051(17)
S2	0	0.7465(5)	0.5304(3)	0.0123(13)	0.012(3)	0.0108(19)	0.014(2)	0	0	–0.0082(17)
S3	0.2980(4)	0.3429(4)	0.5100(3)	0.0136(10)	0.009(2)	0.0149(13)	0.0172(19)	–0.0014(12)	0.0025(15)	–0.0015(12)
S4	0.2884(4)	0.8278(3)	0.7880(2)	0.0123(10)	0.012(2)	0.0149(14)	0.0101(17)	–0.0003(12)	0.0005(15)	0.0039(12)
Na1	0.1629(5)	0.5588(7)	0.6466(4)	0.0241(16)	0.030(3)	0.019(2)	0.023(2)	–0.004(2)	–0.009(2)	–0.0001(19)
Na2	–0.2847(3)	0.5951(4)	0.3474(2)	0.0296(12)	0.037(3)	0.0245(16)	0.0272(18)	0.0019(17)	–0.0017(18)	–0.0021(16)
Na3	0.1620(5)	1.0569(6)	0.6346(3)	0.0189(15)	0.020(3)	0.016(2)	0.020(2)	0.000(2)	0.003(2)	–0.0080(18)
Na4	0	0.3437(8)	–0.0061(3)	0.047(2)	0.055(5)	0.070(4)	0.015(2)	0	0	0.006(3)
Na5	0	0.5682(7)	0.1945(3)	0.043(2)	0.062(5)	0.038(3)	0.028(3)	0	0	–0.002(2)
O1	–0.1014(10)	0.3092(9)	–0.2884(6)	0.020(3)	0.022(6)	0.020(4)	0.019(4)	0.011(4)	–0.005(4)	0.009(4)
O2	0	0.3058(11)	–0.1516(11)	0.023(4)	0.045(10)	0.008(5)	0.015(7)	0	0	–0.004(5)
O3	0	0.0587(12)	–0.2487(9)	0.018(5)	0.023(10)	0.005(6)	0.026(8)	0	0	–0.011(6)
O4	0	0.7930(14)	0.4413(12)	0.026(4)	0.029(9)	0.032(6)	0.017(6)	0	0	0.005(7)
O5	0.1021(10)	0.8055(9)	0.5751(6)	0.019(3)	0.016(6)	0.015(4)	0.026(5)	0.006(4)	–0.003(4)	–0.003(4)
O6	0	0.5570(13)	0.5418(8)	0.011(4)	0.002(8)	0.016(6)	0.016(7)	0	0	–0.012(5)
O7	0.2842(11)	1.1656(9)	0.5337(7)	0.025(3)	0.030(6)	0.014(4)	0.032(5)	0.002(4)	0.003(4)	0.011(4)
O8	0.3313(9)	0.4519(11)	0.5827(6)	0.029(3)	0.034(6)	0.036(5)	0.018(5)	–0.009(4)	0.000(4)	–0.007(4)
O9	0.3815(9)	0.3623(9)	0.4401(7)	0.022(3)	0.031(6)	0.013(3)	0.021(4)	0.001(4)	0.020(5)	0.002(4)
O10	0.1913(8)	0.4117(10)	0.4729(6)	0.018(3)	0.001(5)	0.021(4)	0.031(6)	–0.003(4)	–0.005(4)	–0.003(4)
O11	0.3151(8)	0.9224(10)	0.7094(6)	0.020(3)	0.028(6)	0.017(3)	0.013(4)	–0.005(3)	0.004(4)	0.012(3)
O12	0.2690(11)	0.6495(9)	0.7680(6)	0.022(3)	0.031(6)	0.020(4)	0.014(4)	–0.002(4)	–0.007(4)	0.002(3)
O13	0.3816(8)	0.8470(9)	0.8529(7)	0.020(3)	0.004(5)	0.028(4)	0.027(5)	0.002(4)	0.008(5)	0.010(4)
O14	0.1842(8)	0.9038(11)	0.8273(6)	0.026(3)	0.024(7)	0.018(4)	0.036(6)	0.000(4)	0.005(5)	–0.001(4)
O15	0.5	0.0267(12)	0.4426(10)	0.020(4)	0.018(9)	0.019(5)	0.025(7)	0	0	–0.009(7)
O16	0.5	0.3162(13)	0.2676(8)	0.019(5)	0.024(11)	0.030(7)	0.004(7)	0	0	–0.006(5)
O17	0	0.4687(11)	0.3531(9)	0.014(4)	0.015(8)	0.014(5)	0.012(6)	0	0	0.007(6)
O18	0	0.1800(11)	0.5270(10)	0.016(4)	0.013(9)	0.005(5)	0.029(8)	0	0	–0.002(5)
OW1	–0.3026(6)	0.7878(8)	0.4664(4)	0.031(2)	0.023(5)	0.032(4)	0.038(4)	0.010(3)	–0.013(3)	–0.005(3)
OW2	–0.1336(7)	0.7469(8)	0.2864(5)	0.035(3)	0.028(5)	0.028(3)	0.050(4)	0.001(3)	–0.011(4)	–0.003(3)
OW3	0	0.2653(14)	0.1393(8)	0.034(4)	0.024(7)	0.042(6)	0.035(6)	0	0	0.001(5)
OW4	0	0.8443(18)	0.1325(10)	0.086(7)	0.099(15)	0.090(12)	0.069(11)	0	0	–0.025(9)

Oppenheimerite

	x/a	y/b	z/c	U_{eq}	U^{11}	U^{22}	U^{33}	U^{23}	U^{13}	U^{12}
U	0.76928(2)	0.68331(2)	0.18247(2)	0.01748(11)	0.01705(14)	0.01722(14)	0.01697(14)	0.00016(9)	–0.00489(10)	–0.00610(10)
S1	0.91864(18)	0.05147(18)	0.22112(16)	0.0180(5)	0.0183(6)	0.0186(6)	0.0166(6)	–0.0014(5)	–0.0050(5)	–0.0067(5)
S2	0.65518(18)	0.57316(18)	0.60335(16)	0.0184(5)	0.0180(6)	0.0184(6)	0.0184(7)	–0.0006(5)	–0.0053(5)	–0.0071(5)
Na1	0.9437(3)	0.2298(3)	0.5031(3)	0.0316(11)	0.0248(12)	0.0329(14)	0.0359(14)	0.0037(11)	–0.0082(11)	–0.0145(11)
Na2	0.4542(4)	0.1481(4)	0.2085(3)	0.0496(14)	0.0560(19)	0.0445(17)	0.0348(17)	0.0052(15)	–0.0080(14)	–0.0088(13)
O1	0.7289(5)	0.0807(6)	0.2809(5)	0.0277(18)	0.021(2)	0.035(2)	0.031(2)	0.0056(18)	–0.0067(18)	–0.019(2)
O2	0.0233(6)	0.0826(6)	0.3061(5)	0.0247(17)	0.027(2)	0.028(2)	0.024(2)	–0.0012(18)	–0.0114(18)	–0.0114(18)
O3	0.9877(5)	0.1738(5)	0.0512(5)	0.0257(17)	0.027(2)	0.026(2)	0.016(2)	–0.0062(18)	–0.0034(17)	–0.0028(17)
O4	0.9447(5)	0.8637(5)	0.2320(5)	0.0225(16)	0.022(2)	0.019(2)	0.025(2)	0.0002(16)	–0.0086(17)	–0.0080(16)
O5	0.7573(7)	0.4156(7)	0.6244(6)	0.039(2)	0.045(3)	0.041(3)	0.039(3)	0.021(2)	–0.022(2)	–0.022(2)
O6	0.7367(6)	0.7117(6)	0.6206(5)	0.0283(18)	0.030(2)	0.032(2)	0.025(2)	–0.0093(19)	–0.0058(18)	–0.0130(18)
O7	0.4722(6)	0.5281(6)	0.7232(5)	0.0270(18)	0.027(2)	0.035(2)	0.016(2)	–0.0105(19)	–0.0026(17)	–0.0085(18)
O8	0.6287(5)	0.6469(5)	0.4445(5)	0.0226(16)	0.024(2)	0.022(2)	0.023(2)	0.0001(17)	–0.0097(17)	–0.0086(16)
O9	0.6320(6)	0.8634(6)	0.1240(5)	0.0263(18)	0.028(2)	0.024(2)	0.026(2)	0.0059(19)	–0.0112(19)	–0.0075(18)
O10	0.9082(6)	0.5028(6)	0.2405(5)	0.0262(18)	0.027(2)	0.021(2)	0.024(2)	0.0034(18)	–0.0070(18)	–0.0040(18)
OW1	0.7462(6)	0.6218(6)	0.9580(5)	0.0324(19)	0.033(2)	0.044(3)	0.022(2)	–0.010(2)	–0.0021(19)	–0.018(2)
OW2	0.6575(6)	0.1095(6)	0.5649(5)	0.0294(19)	0.025(2)	0.033(2)	0.034(2)	0.0032(19)	–0.0090(19)	–0.018(2)
OW3	0.6772(7)	0.2985(6)	0.9665(5)	0.034(2)	0.038(3)	0.034(3)	0.028(2)	0.005(2)	–0.014(2)	–0.008(2)

TABLE 5. Selected bond distances (Å) and angles (°) for fermiite and oppenheimerite.

Fermiite									
Na1–O1	2.319(10)	Na2–OW2	2.345(8)	Na3–O7	2.284(12)	Na4–O2	2.250(17)	Na5–OW4	2.372(15)
Na1–O5	2.342(10)	Na2–O12	2.365(9)	Na3–O5	2.291(10)	Na4–OW3	2.312(13)	Na5–OW3	2.529(13)
Na1–O12	2.355(12)	Na2–OW1	2.380(7)	Na3–O11	2.391(10)	Na4–OW1(×2)	2.591(8)	Na5–OW2(×2)	2.542(8)
Na1–O8	2.376(12)	Na2–O9	2.586(9)	Na3–O1	2.419(10)	Na4–O9(×2)	2.828(10)	Na5–O17	2.553(14)
Na1–O6	2.510(10)	Na2–O1	2.593(10)	Na3–O3	2.623(11)	Na4–O8(×2)	2.903(11)	Na5–O8(×2)	2.637(11)
Na1–O16	2.850(11)	Na2–O10	2.646(9)	Na3–O18	2.708(11)	Na4–O15	3.019(13)	<Na5–O>	2.545
Na1–O10	2.923(11)	Na2–O2	2.666(5)	<Na3–O>	2.453	<Na4–O>	2.692		
<Na1–O>	2.525	<Na2–O>	2.512						
				S1–O1(×2)	1.448(11)	S2–O4	1.414(18)		
U1–O15	1.756(14)	U2–O17	1.741(12)	S1–O2	1.489(16)	S2–O5(×2)	1.466(11)	Hydrogen bonds	
U1–O16	1.763(12)	U2–O18	1.762(13)	S1–O3	1.518(10)	S2–O6	1.502(11)	OW1–O15	3.022(9)
U1–O14(×2)	2.305(10)	U2–O13(×2)	2.346(9)	<S1–O>	1.476	<S2–O>	1.462	OW1–O2	3.046(12)
U1–O9(×2)	2.420(9)	U2–O6	2.422(11)					OW2–O4	2.876(17)
U1–O3	2.427(11)	U2–O10(×2)	2.426(9)	S3–O7	1.451(8)	S4–O11	1.451(9)	OW2–O17	2.888(11)
<U1–O_{ap}>	1.760	<U2–O_{ap}>	1.752	S3–O8	1.460(10)	S4–O12	1.455(8)	OW3–O11	2.851(12)
<U1–O_{eq}>	2.375	<U2–O_{eq}>	2.393	S3–O9	1.465(11)	S4–O13	1.493(11)	OW3–O8	3.113(13)
				S3–O10	1.488(10)	S4–O14	1.497(10)	OW4–OW2	2.942(15)
				<S3–O>	1.466	<S4–O>	1.474	OW4–O7	2.972(15)
Oppenheimerite									
U–O9	1.768(5)	S1–O1	1.459(4)	Na1–OW2	2.353(5)	Na2–OW2	2.322(4)	Hydrogen bonds	
U–O10	1.778(4)	S1–O2	1.461(6)	Na1–O5	2.406(6)	Na2–OW3	2.344(5)	OW1–O2	2.911(5)
U–O8	2.332(4)	S1–O3	1.487(4)	Na1–O6	2.418(5)	Na2–O6	2.439(6)	OW1–OW3	2.719(8)
U–O3	2.370(3)	S1–O4	1.498(5)	Na1–O2	2.535(4)	Na2–O1	2.467(6)	OW2–O1	2.752(8)
U–O7	2.383(5)	<S1–O>	1.476	Na1–O2	2.552(6)	Na2–OW1	2.727(6)	OW2–O8	2.882(6)
U–O4	2.410(5)			Na1–O10	2.719(5)	Na2–O9	2.878(6)	OW3–O1	3.015(7)
U–OW1	2.515(6)	S2–O5	1.437(5)	Na1–O4	2.815(6)	<Na2–O>	2.530	OW3–O5	2.938(8)
<U–O_{ap}>	1.773	S2–O6	1.453(6)	<Na1–O>	2.543				
<U–O_{eq}>	2.402	S2–O7	1.494(4)						
		S2–O8	1.506(5)						
		<S2–O>	1.473						

TABLE 6. Bond-valence analysis for fermiite and oppenheimerite. Values are expressed in valence units.*

Fermiite	O1	O2	O3	O4	O5	O6	O7	O8	O9	O10	O11	O12	O13	O14	O15	O16	O17	O18	OW1	OW2	OW3	OW4	Σ_c
Na1	0.22				0.20	0.13 ×2↓		0.19		0.04		0.20				0.05 ×2↓							1.03
Na2	0.10	0.09 ×2↓							0.11	0.09		0.19							0.19	0.20			0.97
Na3	0.17		0.10 ×2↓		0.24		0.24				0.18							0.08 ×2↓					1.01
Na4		0.26						0.05 ×2→	0.06 ×2→						0.03				0.10 ×2→		0.22		0.93
Na5								0.09 ×2→									0.12			0.12 ×2→	0.12	0.19	0.85
U1			0.48						0.49 ×2→					0.61 ×2→	1.77	1.74							6.19
U2						0.49				0.49 ×2→			0.57 ×2→				1.82	1.75					6.18
S1	1.61 ×2→	1.44	1.33																				5.99
S2				1.76	1.53 ×2→	1.39																	6.21
S3							1.60	1.56	1.54	1.44													6.14
S4											1.60	1.58	1.42	1.41									6.01
H1a															0.09				0.91				1.00
H1b		0.08																	0.92				1.00
H2a				0.16																0.84			1.00
H2b																	0.15			0.85			1.00
H3a											0.16										0.84		1.00
H3b								0.05													0.95		1.00
H4a																				0.13		0.87	1.00
H4b							0.11															0.89	1.00
Σ_a	2.10	1.96	2.01	1.92	1.97	2.14	1.95	1.94	2.20	2.06	2.10	1.97	1.99	2.02	1.89	1.84	2.09	1.91	2.12	2.14	2.13	1.95	

(continued)

TABLE 6 (*contd.*)

	Oppenheimerite													
	O1	O2	O3	O4	O5	O6	O7	O8	O9	O10	OW1	OW2	OW3	Σ_c
Na1		0.12		0.06	0.17	0.17				0.07		0.20		0.91
		0.12												
Na2	0.15					0.16			0.05		0.07	0.22	0.20	0.85
U1			0.54	0.50			0.53	0.58	1.73	1.69	0.41			5.98
S1	1.56	1.55	1.45	1.41										5.97
S2					1.66	1.59	1.42	1.38						6.05
H1a		0.14									0.86			1.00
H1b											0.80		0.20	1.00
H2a	0.19											0.81		1.00
H2b								0.15				0.85		1.00
H3a	0.09												0.91	1.00
H3b					0.13								0.87	1.00
Σ_a	1.99	1.93	1.99	1.97	1.96	1.92	1.95	2.11	1.78	1.76	2.14	2.08	2.18	

Multiplicity is indicated by ×↓→. S^{6+}–O bond-valence parameter from Brown and Altermatt (1985); Na^{+}–O from Wood and Palenik (1999); U^{6+}–O from Burns *et al.* (1997); Hydrogen-bond strengths based on O–O bond lengths from Brown and Altermatt (1985).

2001) in the *CrystalClear* software suite. The oppenheimerite structure was solved by direct methods using *SIR2004* (Burla *et al*., 2005).

Both structures were refined using the software *Jana2006* (Petříček *et al*., 2006, 2014) with the full-matrix least-squares refinement based on F^2. For both structure refinements, difference Fourier syntheses failed to locate the H atom positions. Data collection and refinement details are given in Table 3, atom coordinates and displacement parameters in Table 4, selected bond distances in Table 5 and bond-valence analyses in Table 6.

Description and discussion of the structures

In the structures of fermiite and oppenheimerite, the U sites are surrounded by seven O atom sites forming squat pentagonal bipyramids. This is the most typical coordination for U^{6+}, particularly in uranyl sulfates (Krivovichev, 2010, 2013), where the two short apical bonds of the bipyramid constitute the uranyl group. The bond lengths in the U^{6+}-coordination polyhedron in both structures (fermiite: $\langle U1–O_{ap}\rangle$ = 1.793, $\langle U1–O_{eq}\rangle$ = 2.401, $\langle U2–O_{ap}\rangle$ = 1.749, $\langle U2–O_{eq}\rangle$ = 2.391; oppenheimerite: $\langle U–O_{ap}\rangle$ = 1.770, $\langle U–O_{eq}\rangle$ = 2.400 Å) are consistent with the most typical lengths observed for [7]-coordinated U^{6+} (Burns *et al.*, 1997). In the fermiite structure, all five of the equatorial O atoms also participate in SO_4 tetrahedra, while in the oppenheimerite structure, four of the five equatorial O atoms also participate in SO_4 tetrahedra and the fifth is an H_2O group. In both structures, adjacent pentagonal bipyramids are linked to one another via two bridging SO_4 groups forming infinite chains. The $[(UO_2)(SO_4)_3]^{4–}$ chain in fermiite is parallel to [100] and the $[(UO_2)(SO_4)_2(H_2O)]^{2–}$ chain in oppenheimerite is parallel to $[11\bar{1}]$. In both structures, the chains are linked by bonds involving Na–O polyhedra to form a framework. The structures are described in more detail below.

Fermiite

In the structure of fermiite (Fig. 9), there are four different S sites (S1, S2, S3 and S4). The U1 bipyramid links to one S1, two S3 and two S4 tetrahedra; the U2 bipyramid links to one S2, two S3 and two S4 tetrahedra. The S3–S4 pairs of tetrahedra link the U1 and U2 bipyramids to form the infinite chain parallel to [100] that is decorated with S1 and S2 tetrahedra, yielding a $[(UO_2)(SO_4)_3]^{4–}$ structural unit (Fig. 10). Four different Na atoms (Na1, Na2, Na3 and Na4) form bonds to O atoms in the polyhedral chains, thereby linking them into a three-dimensional framework. Four different H_2O groups (OW1, OW2, OW3 and OW4) between the chains also participate in Na coordination and form hydrogen bonds that further link the framework.

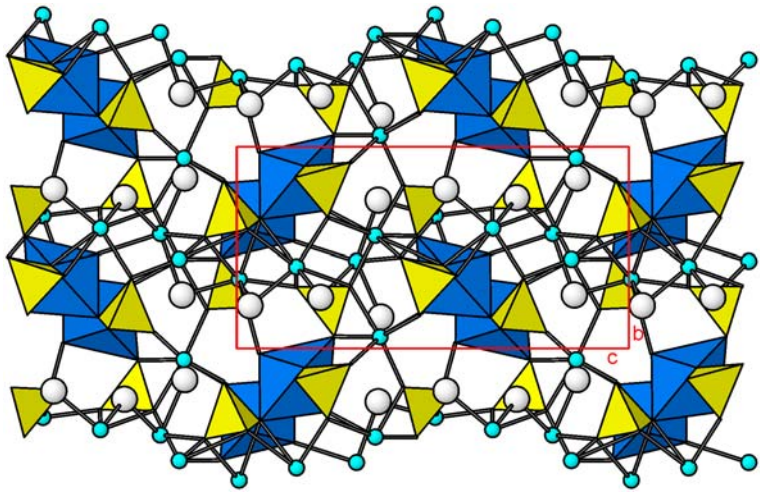

FIG. 9. The structure of fermiite viewed down [100], the chain direction. UO_7 bipyramids are dark blue, SO_4 tetrahedra are yellow, Na atoms are light blue spheres and O atoms of isolated H_2O groups are white spheres. The unit is cell shown by red lines.

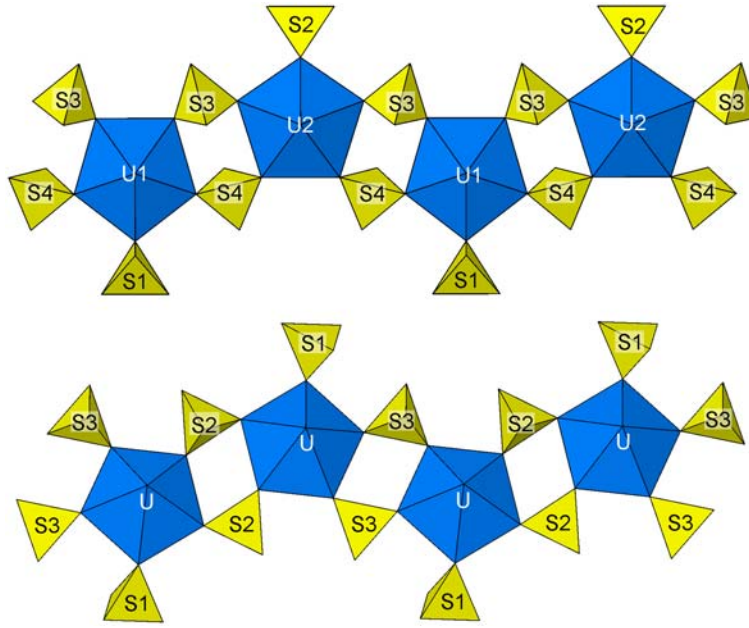

FIG. 10. The uranyl sulfate chains in fermiite (top) and meisserite (bottom).

The hydrogen bonds listed in Table 5 were chosen based upon a consideration of O–O distance, hydrogen-bond geometry and bond-valence balance.

The same $[(UO_2)(SO_4)_3]^{4-}$ structural unit has been found in the structure of meisserite, $Na_5(UO_2)(SO_4)_3(SO_3OH)(H_2O)$ (Plášil *et al.*, 2013), which occurs in the same assemblage at the Blue Lizard mine. The chains in the two structures are topologically identical and differ only in relatively minor geometrical distortions

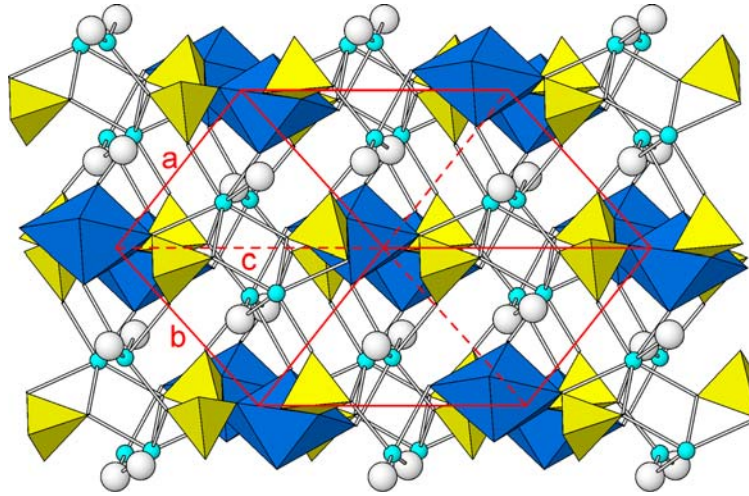

FIG. 11. The structure of oppenheimerite viewed down [11$\bar{1}$], the chain direction. UO_7 bipyramids are dark blue, SO_4 tetrahedra are yellow, Na atoms are light blue spheres and O atoms of isolated H_2O groups are white spheres. The unit cell is shown by red lines.

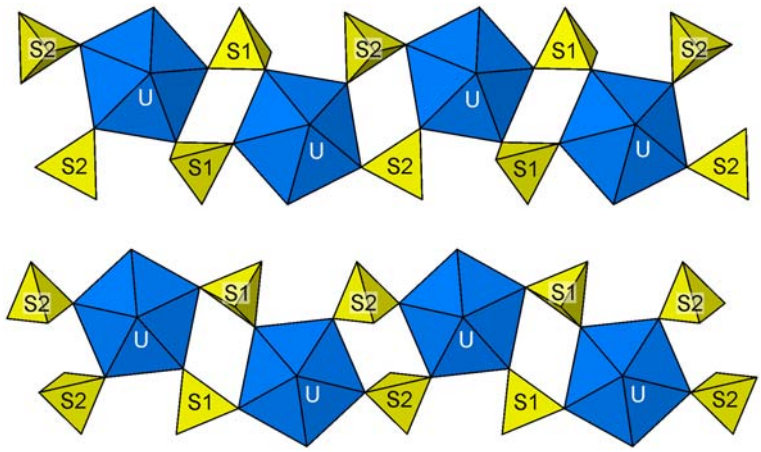

FIG. 12. The uranyl sulfate chains in oppenheimerite (top) and bobcookite (bottom).

and the orientations of the decorating SO_4 groups (Fig. 10). A topologically identical chain was also found in the structure of synthetic $Na_3Tl_5[(UO_2)(MoO_4)_3]_2(H_2O)_3$ (Krivovichev and Burns, 2003).

Oppenheimerite

In the structure of oppenheimerite (Fig. 11), there are two different S sites (S1 and S2). The U bipyramid links to two S1 and two S2 tetrahedra. The S1–S1 and S2–S2 pairs of tetrahedra link the U bipyramids to form the infinite $[(UO_2)(SO_4)_2(H_2O)]$ chain structural unit running along $[11\bar{1}]$. Two different Na atoms (Na1 and Na2) form bonds to O atoms in the polyhedral chains, thereby linking them into a three-dimensional framework. Two different H_2O groups (OW2 and OW3) between the chains also participate in Na coordination and form hydrogen bonds that further link the framework.

Similar $[(UO_2)(SO_4)_2(H_2O)]^{2-}$ chains are found in the structures of bobcookite (Kampf *et al*. 2015*b*), synthetic $K_2[(UO_2)(SO_4)_2(H_2O)](H_2O)$ (Ling *et al.*, 2010) and synthetic $Mn(UO_2)(SO_4)_2(H_2O)_5$ (Tabachenko *et al.*, 1979). The oppenheimerite and bobcookite chains are compared in Fig. 12. The chains in these two structures are geometrical isomers.

Acknowledgements

The Editorial Board Member Stuart Mills, Structures Editor Peter Leverett and two anonymous reviewers are thanked for their constructive comments on the manuscript. Atali A. Agakhanov and Ladislav Lapčák are thanked for their assistance with the chemistry and Raman measurements, respectively. A portion of this study was funded by the John Jago Trelawney Endowment to the Mineral Sciences Department of the Natural History Museum of Los Angeles County. This research was also financially supported by GAČR post-doctoral Grant no. 13-31276P to J.P. Further support was provided by long-term project DKRVO 2014/02 of the Ministry of Culture of the Czech Republic (National Museum 000232782) to J.Č.

References

Bartlett, J.R. and Cooney, R.P. (1989) On the determination of uranium-oxygen bond lengths in dioxouranium(VI) compounds by Raman spectroscopy. *Journal of Molecular Structure*, **193**, 295–300.

Brown, I.D. and Altermatt, D. (1985) Bond-valence parameters from a systematic analysis of the inorganic crystal structure database. *Acta Crystallographica*, **B41**, 244–247.

Burla, M.C., Caliandro, R., Camalli, M., Carrozzini, B., Cascarano, G.L., De Caro, L., Giacovazzo, C., Polidori, G. and Spagna, R. (2005) *SIR2004*: an improved tool for crystal structure determination and refinement. *Journal of Applied Crystallography*, **38**, 381–388.

Burns, P.C., Ewing, R.C. and Hawthorne, F.C. (1997) The crystal chemistry of hexavalent uranium: polyhedron geometries, bond-valence parameters, and polymerization of polyhedra. *The Canadian Mineralogist*, **35**, 1551–1570.

Chenoweth, W.L. (1993) *The geology and production history of the uranium deposits in the White Canyon mining district, San Juan County, Utah.*

Miscellaneous Publication 93-3, Utah Geological Survey, Salt Lake City, Utah, USA.

Higashi, T. (2001) *ABSCOR.* Rigaku Corporation, Tokyo.

Kampf, A.R., Plášil, J., Kasatkin, A.V. and Marty, J. (2014) Belakovskiite, $Na_7(UO_2)(SO_4)_4(SO_3OH)(H_2O)_3$, a new uranyl sulfate mineral from the Blue Lizard mine, San Juan County, Utah, USA. *Mineralogical Magazine*, **78**, 639–649.

Kampf, A.R., Kasatkin, A.V., Čejka, J. and Marty, J. (2015*a*) Plášilite, $Na(UO_2)(SO_4)(OH)\cdot 2H_2O$, a new uranyl sulfate mineral from the Blue Lizard mine, San Juan County, Utah, USA. *Journal of Geosciences*, **60**, 1–10.

Kampf, A.R., Plášil, J., Kasatkin, A.V. and Marty, J. (2015*b*) Bobcookite, $NaAl(UO_2)_2(SO_4)_4\cdot 18H_2O$ and wetherillite, $Na_2Mg(UO_2)_2(SO_4)_4\cdot 18H_2O$, two new uranyl sulfate minerals from the Blue Lizard mine, San Juan County, Utah, USA. *Mineralogical Magazine*, **79**, 695–714.

Kasatkin, A.V., Nestola, F., Plášil, J., Marty, J., Belakovskiy, D.I., Agakhanov, A.A., Mills, S.J., Pedron, D., Lanza, A., Favaro, M., Bianchin, S., Lykova, I.S., Goliáš, V. and Birch, W.D. (2013) Manganoblödite, $Na_2Mn(SO_4)_2\cdot 4H_2O$, and cobaltoblödite, $Na_2Co(SO_4)_2\cdot 4H_2O$: two new members of the blödite group from the Blue Lizard mine, San Juan County, Utah, USA. *Mineralogical Magazine*, **77**, 367–383.

Krivovichev, S.V. (2010) Actinyl compounds with hexavalent elements (S, Cr, Se, Mo) – structural diversity, nanoscale chemistry, and cellular automata modeling. *European Journal of Inorganic Chemistry*, **2010**, 2594–2603.

Krivovichev, S.V. (2013) Crystal chemistry of uranium oxides and minerals. Pp. 611–640 in: *Comprehensive Inorganic Chemistry II, Vol 2* (J. Reedijk and K. Poeppelmeier, editors). Elsevier, Oxford.

Krivovichev, S.V. and Burns, P.C. (2003) Crystal chemistry of uranyl molybdates. VIII. Crystal structures of $Na_3Tl_3[(UO_2)(MoO_4)_4]$, $Na_{13-x}Tl_{3+x}[(UO_2)(MoO_4)_3]_4(H_2O)_{6+x}$ ($x = 0.1$), $Na_3Tl_5[(UO_2)(MoO_4)_3]_2(H_2O)_3$ and $Na_2[(UO_2)(MoO_4)_2](H_2O)_4$. *The Canadian Mineralogist*, **41**, 707–719.

Libowitzky, E. (1999) Correlation of O–H stretching frequencies and O–H···O hydrogen bond lengths in minerals. *Monatshefte für Chemie*, **130**, 1047–1059.

Ling, J., Sigmon, G.E., Ward, M., Roback, N. and Burns, P.C. (2010) Syntheses, structures, and IR spectroscopic characterization of new uranyl sulfate/selenate 1D-chain, 2D-sheet and 3D framework. *Zeitschrift für Kristallographie*, **225**, 230–239.

Mandarino, J.A. (1976) The Gladstone-Dale relationship – Part 1: derivation of new constants. *The Canadian Mineralogist*, **14**, 498–502.

Mandarino, J.A. (2007) The Gladstone–Dale compatibility of minerals and its use in selecting mineral species for further study. *The Canadian Mineralogist*, **45**, 1307–1324.

Palatinus, L. (2013) The charge flipping algorithm in crystallography. *Acta Crystallographica*, **B69**, 1–16.

Palatinus, L. and Chapuis, G. (2007) Superflip – A computer program for the solution of crystal structures by charge flipping in arbitrary dimensions. *Journal of Applied Crystallography*, **40**, 451–456.

Palatinus, L. and van der Lee, A. (2008) Symmetry determination following structure solution in *P*1. *Journal of Applied Crystallography*, **41**, 975–984.

Petříček, V., Dušek, M. and Palatinus, L. (2006) *Jana2006.* The Crystallographic Computing System. Institute of Physics, Prague.

Petříček, V., Dušek, M. and Palatinus, L. (2014) Crystallographic computing system Jana 2006: general features. *Zeitschrift für Kristallographie*, **229**, 345–352.

Plášil, J. (2014) Oxidation–hydration weathering of uraninite: the current state-of-knowledge. *Journal of Geosciences*, **59**, 99–114.

Plášil, J., Buixaderas, E., Čejka, J., Sejkora, J., Jehlička, J. and Novák, M. (2010) Raman spectroscopic study of the uranyl sulphate mineral zippeite: low wavenumber and U–O stretching regions. *Analytical and Bioanalytical Chemistry*, **397**, 2703–2715.

Plášil, J., Kampf, A.R., Kasatkin, A.V., Marty, J., Škoda, R., Silva, S. and Čejka, J. (2013) Meisserite, $Na_5(UO_2)(SO_4)_3(SO_3OH)(H_2O)$, a new uranyl sulfate mineral from the Blue Lizard mine, San Juan County, Utah, USA. *Mineralogical Magazine*, **77**, 2975–2988.

Plášil, J., Kampf, A.R., Kasatkin, A.V. and Marty, J. (2014) Bluelizardite, $Na_7(UO_2)(SO_4)_4Cl(H_2O)_2$, a new uranyl sulfate mineral from the Blue Lizard mine, San Juan County, Utah, USA. *Journal of Geosciences*, **59**, 145–158.

Tabachenko, V.V., Serezhkin, V.I., Serezhkina, L.B. and Kovba, L.M. (1979) Crystal structure of manganese sulfatouranylate $MnUO_2(SO_4)_2(H_2O)_5$. *Koordinatsionnaya Khimiya*, **5**, 1563–1568.

Volkovich, V.A., Griffiths, T.R., Fray, D.J. and Fields, M. (1998) Vibrational spectra of alkali metal Li, Na and K uranates and consequent assignment of uranate ion site symmetry. *Vibrational Spectroscopy*, **17**, 83–91.

Wood, R.M. and Palenik, G.J. (1999) Bond valence sums in coordination chemistry. Sodium-oxygen complexes. Inorganic Chemistry, **38**, 3926–3930.